

Precursor-Induced Hydrothermal Synthesis of Flowerlike Cupped-End Microrod Bundles of ZnO

Changlong Jiang, Wangqun Zhang, Guifu Zou, Weicao Yu, and Yitai Qian*

Structure Research Laboratory and Department of Chemistry, University of Science and Technology of China, Hefei, Anhui, 230026, People's Republic of China

Received: July 27, 2004; In Final Form: November 1, 2004

Flowerlike cupped-end ZnO microrod bundles have been hydrothermally synthesized from precursor $\text{ZnCl}_2 \cdot (\text{N}_2\text{H}_4)_2$ in sheet shape at 140 °C for 12 h; under the same conditions using the same precursor in rod shape, uniform ZnO nanorods were obtained. XRD pattern indicated the sample is ZnO with hexagonal cell constants $a = 3.251 \text{ \AA}$ and $c = 5.206 \text{ \AA}$. FE-SEM and TEM show the formation process of the ZnO sample. HRTEM revealed that the flowerlike cupped-end ZnO microrod bundles grow along the [101] axis. The UV emission peak at $\sim 396 \text{ nm}$ and the blue band emission peak at $\sim 469 \text{ nm}$ were observed by PL spectra. A possible formation mechanism was proposed.

Introduction

Recently, much effort has been explored for rational control over size, shape, and dimensionality of nanocrystallines¹ because these facts are technically important for optical, electrical, and other properties.² ZnO, which has shown a wide range of technological applications including transparent conducting electrodes of solar cells, flat panel displays, surface acoustic wave devices, and chemical sensors, is a potentially useful semiconductor with a direct band gap of 3.37 eV.^{3–7} Since Yang et al. reported ZnO nanowire array nanoclusters,⁸ vast interest has been devoted to the synthesis of ZnO with controlled structures. The vapor transport and condensation (CVTC) process⁹ has been proved an effective route to the synthesis of ZnO with different shapes such as nanoribbons,¹⁰ nanowires arrays,¹¹ tetrapods,¹² nanotubes,¹³ comblike structures,¹⁴ towerlike structures,¹⁵ single-crystal columns array,¹⁶ and nanowire–nanobelt junction arrays.¹⁷ Novel hierarchical ZnO nanostructures with 6-, 4-, 2-fold symmetries¹⁸ and nanonails and nanobridges have also been grown on In_2O_3 nanowire cores.¹⁹ Recently, ZnO microrods have been prepared through crystalline ZnO template²⁰ and decomposing hexamethylenetetramine (HMT) with zinc nitrate ($\text{Zn}(\text{NO}_3)_2$) in aqueous solution.²¹

In this study, we reported the hydrothermal synthesis of flowerlike cupped-end ZnO microrod bundles at 140 °C for 12 h from precursor $\text{ZnCl}_2 \cdot (\text{N}_2\text{H}_4)_2$ in sheet shape. Under the same conditions using the same precursor in rod shape, uniform ZnO nanorods have been obtained.

Experimental Section

All of the reagents (analytical grade purity) were purchased from Shanghai Chemical Reagents Co. and were used without further purification.

Synthesis of the Precursor. In a typical experiment, 1.36 g of anhydrous ZnCl_2 was dissolved in 40 mL of deionized water, and then 5 mL of hydrazine hydrate ($\text{N}_2\text{H}_4 \cdot \text{H}_2\text{O}$) was added to the above solution under continuous stirring for 4 h. A white

precipitate formed immediately, which implied the formation of $\text{ZnCl}_2 \cdot (\text{N}_2\text{H}_4)_2$, and the resulting product (A) was filtered off, washed with absolute ethanol and distilled water several times, and dried in a vacuum at 60 °C for 4 h. Sample (B) was obtained by transforming the above mixture into a 50 mL Teflon-lined stainless steel autoclave, which was sealed and maintained at 100 °C for 4 h.

Synthesis of Flowerlike Cupped-End ZnO Microrod Bundles. First, 0.01 mol of precursor (A) and 30 mL of deionized water were loaded into a 50 mL Teflon-lined stainless steel autoclave, and 3 mL of ammonia (25 wt %) was added, and then the autoclave was filled with distilled water up to 90% of the total volume, sealed, and kept at 140 °C for 12 h. The resulting white product was filtered off, washed with absolute ethanol and distilled water several times, and finally dried in a vacuum at 60 °C for 4 h.

For the preparation of uniform nanorods, 0.01 mol of precursor (B) was substituted for (A) in the above experiment under the same conditions.

Characterization. The phase purity of the as-prepared products was determined by X-ray diffraction (XRD) using a Philips X'Pert PRO SUPER X-ray diffractometer equipped with graphite monochromatized Cu K α radiation ($\lambda = 1.541874 \text{ \AA}$). Field-emission scanning electron microscopy (FE-SEM) was applied to investigate the morphology, which was carried out with a field-emission scanning electron microanalyzer (JEOL-6300F, 15 kV). The nano-/microstructure of the ZnO products were further observed by transmission electron microscopy (TEM) and high-resolution transmission electron microscopy (HRTEM), which were taken on a Hitachi model H-800 and a JEOL-2010 TEM both with an accelerating voltage of 200 kV, respectively. The photoluminescence (PL) spectrum was recorded using a Hitachi 850 fluorescence spectrophotometer.

Results and Discussion

Figure 1a shows the XRD pattern of the precursor $\text{ZnCl}_2 \cdot (\text{N}_2\text{H}_4)_2$ with monoclinic cell constants ($a = 8.970 \text{ \AA}$, $b = 7.921 \text{ \AA}$, $c = 4.132 \text{ \AA}$, and $\beta = 105.50^\circ$), in good agreement with the reported data (JCPDS 72-0502, $a = 8.990 \text{ \AA}$, $b = 7.920 \text{ \AA}$, $c = 4.130 \text{ \AA}$, and $\beta = 105.50^\circ$). Figure 1b is the typical XRD

* To whom correspondence should be addressed. Fax: +86-551-3607402. E-mail: ytqian@ustc.edu.cn.

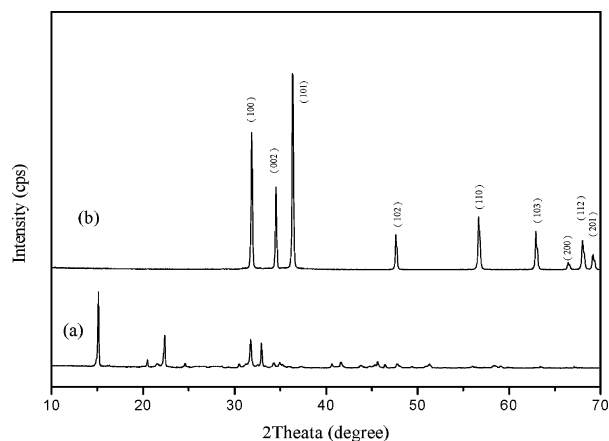


Figure 1. XRD patterns of (a) the precursor $\text{ZnCl}_2(\text{N}_2\text{H}_4)_2$, and (b) ZnO sample obtained from the precursor.

pattern of as-prepared ZnO sample with lattice constants ($a = 3.251 \text{ \AA}$, $c = 5.206 \text{ \AA}$); all of the peaks could be indexed to hexagonal ZnO and close to the reported data (JCPDS 79-2205, $a = 3.250 \text{ \AA}$, $c = 5.207 \text{ \AA}$). No impurities could be detected in this pattern, which implies hexagonal phase ZnO could be obtained under the current synthetic route.

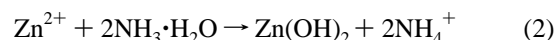
Figure 2a is the FE-SEM image of the precursor $\text{ZnCl}_2(\text{N}_2\text{H}_4)_2$ obtained at room temperature, which display nanosheets with the diameter of 300–400 nm and thickness of 30 nm. In Figure 2b, the as-obtained ZnO sample shows a typical hexagonal morphology and self-assembles into flowerlike microrod bundles; especially the microrods have a cupped-end. The similar shape of ZnO structures has been previously reported to be dependent on the growth pressure in the vapor-phase-deposition process; when the pressure was decreased, the ZnO columns became tubelike structures.²²

Figure 2d is a typical TEM pattern of the cupped-end ZnO microrod bundles; a flowerlike structure is observed. A hexagonal nano-ring with the diameter of 250 nm is shown in Figure 2e, which might be split from the transect of the microrod. Figure 2f shows the assembling ZnO microrod bundles; two hollow ends of the microrods are clearly displayed, but the middle part remains stuffed, in good agreement with the FE-SEM observation. The HRTEM lattice fringes image and SAED (selected area electron diffraction) pattern shown in Figure 2g reveal that, in this region, the microrods possess a single-crystal

hexagonal structure; the image also confirms that the microrod bundles grow along the [101] direction (indicated with the arrow).

By adjusting the experiment condition, uniform ZnO nanorods with the diameters ranging from 40 to 60 nm have been prepared from the precursor $\text{ZnCl}_2(\text{N}_2\text{H}_4)_2$ in rod shape. Figure 3a shows the rodlike precursor prepared at 100 °C for 4 h with the diameter of about 300 nm and the length above 5 μm . In Figure 3b, the ZnO nanorods display a flowerlike structure similar to the precursor in Figure 3a; while prolonging the reaction time to 24 h, the final sample shows hexagonal microrods and the diameter increases to 250 nm. A typical tripod and polypod structure of ZnO nanorods with a diameter of about 50 nm are shown in Figure 3c and d; a similar structure was also noticed in the precursor in Figure 3a. For comparison, we also used ZnCl_2 as the starting material under the same experimental conditions; the obtained ZnO has whiskers with a diameter ranging from 200 nm to 1 μm instead of uniform nanorods with a diameter of 40–60 nm.

The overall reaction in the current system could be simply formulated as follows:



ZnCl_2 and hydrazine hydrate ($\text{N}_2\text{H}_4 \cdot \text{H}_2\text{O}$) could form the coordination compound $\text{ZnCl}_2(\text{N}_2\text{H}_4)_2$ in aqueous solution, Zn^{2+} salt solution reacts with ammonia to form $\text{Zn}(\text{OH})_2$ precipitate,²³ and finally ZnO may be obtained by hydrothermal treatment of $\text{Zn}(\text{OH})_2$.

In the current synthesis route, the obtained ZnO samples synthesized from the precursor in different shapes might be formed through a dissolution-recrystallization-decomposition-growth process. First, $\text{ZnCl}_2(\text{N}_2\text{H}_4)_2$ dissolved and reacted with ammonia to form $\text{Zn}(\text{OH})_2$, then the $\text{Zn}(\text{OH})_2$ rapidly decomposed into ZnO nanoparticles, and finally ZnO with different morphologies was obtained by the oriented attachment of the newly formed ZnO nanoparticles. This proposed formation mechanism is similar to the solution-solid (SS) process. In the early stage of the synthesis, the dissolution of $\text{ZnCl}_2(\text{N}_2\text{H}_4)_2$ is

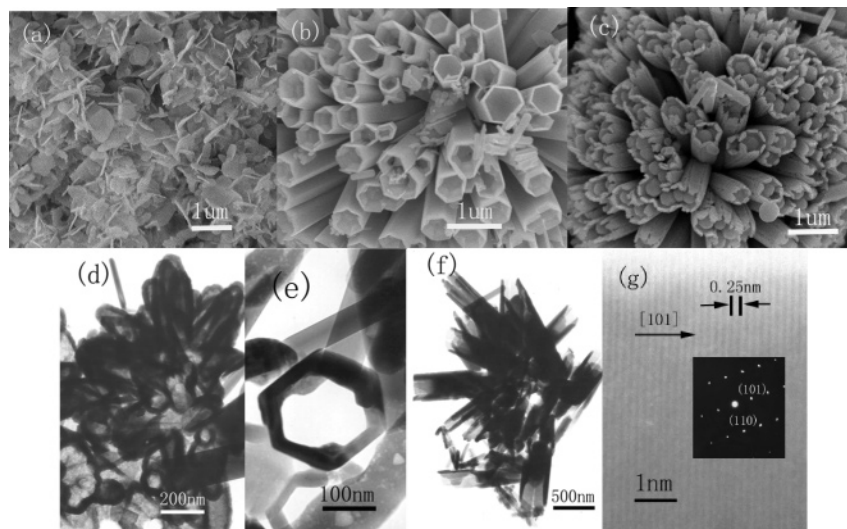


Figure 2. FE-SEM images of (a) precursor $\text{ZnCl}_2(\text{N}_2\text{H}_4)_2$ obtained at room temperature, ZnO samples obtained at 140 °C and 12 h (b), 3 h (c), and (d–g) TEM and HRTEM patterns of the flowerlike cupped-end ZnO microrod bundles.

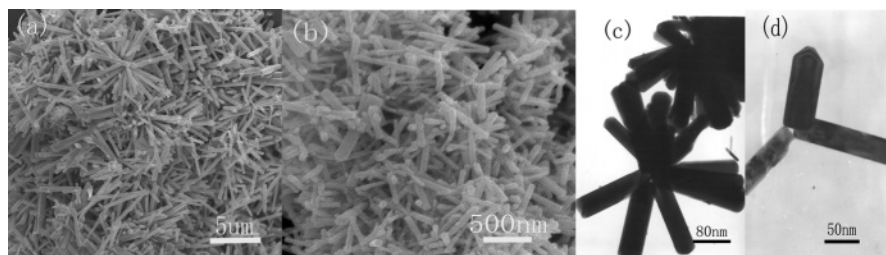


Figure 3. FE-SEM patterns of precursor $\text{ZnCl}_2(\text{N}_2\text{H}_4)_2$ obtained at 100 °C for 4 h (a), ZnO nanorods prepared at 140 °C for 12 h (b), and TEM (c,d) images of ZnO nanorods.

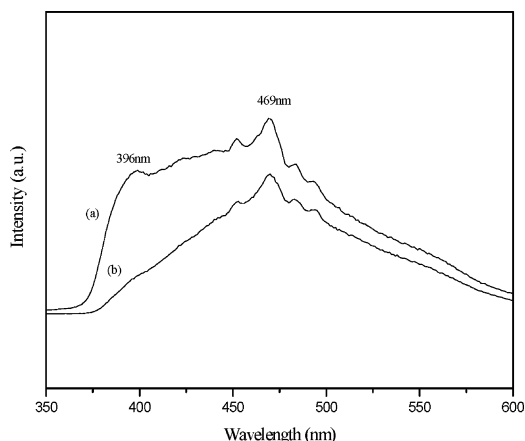


Figure 4. PL spectra ($\lambda_{\text{ex}} = 325$ nm) of (a) ZnO nanorods and (b) flowerlike microrod bundles.

very slow in contrast to the direct decomposition of ZnCl_2 in aqueous solution, so the growth of ZnO sample was controlled by the step of the dissolution of $\text{ZnCl}_2(\text{N}_2\text{H}_4)_2$. Thus, the nucleation of ZnO nanoparticles was also very slow so that the quantity of the newly formed ZnO nanoparticles under hydrothermal system was maintained at a low level, which provided a favorable condition for the growth of ZnO sample. In addition, with the same precursor in different shapes, flowerlike cupped-ended microrod bundles and uniform nanorods of ZnO were prepared under hydrothermal conditions, respectively. The shape of the precursor may play a very important role for the final ZnO product; the specific influence of the shape of the precursor on the final morphology of the ZnO product is not yet clear and warrants further investigation, and a related study is underway.

Photoluminescence (PL) spectra of the ZnO sample were measured and are shown in Figure 4. The two emission peaks of a weak peak at ~ 396 nm and a broad peak at ~ 469 nm were observed, which were assigned to the UV emission and blue band emission, respectively.²⁴ The UV emission should be attributed to near band-edge emission of the wide band gap of ZnO; the mechanism of blue band emission is not yet clear.²⁵

Conclusions

In summary, we have hydrothermally synthesized flowerlike cupped-end microrod bundles from the precursor $\text{ZnCl}_2(\text{N}_2\text{H}_4)_2$ in sheet shape; uniform ZnO nanorods were obtained using the same precursor in rod shape under the same conditions. The shape of the precursor plays a very important role in the final morphology of ZnO sample. PL spectra recorded the optical properties, and a blue band emission peak at ~ 469 nm was observed. A possible formation mechanism has also been proposed.

Acknowledgment. Financial support from the National Natural Science Funds and the 973 Projects of China is gratefully acknowledged.

Supporting Information Available: Figure 1S (FE-SEM images of the depiction of flowerlike cupped-end ZnO microrod bundles obtained at 140 °C for 12 h (a), 6 h (b), and 9 h (c)) and Figure 2S (FE-SEM image of 250 nm-diameter uniform ZnO microrods obtained at 140 °C for 24 h (a), TEM pattern of the 50 nm-diameter uniform ZnO nanorods obtained at 140 °C for 12 h (b), and FE-SEM pattern of ZnO whiskers with the diameter ranging from 200 nm to 1 μm obtained using ZnCl_2 as the starting material (c)). This material is available free of charge via the Internet at <http://pubs.acs.org>.

References and Notes

- (1) Xia, Y.; Yang, P.; Sun, Y.; Wu, Y.; Mayer, B.; Gates, B.; Yin, Y.; Kim, F.; Yan, H. *Adv. Mater.* **2003**, *15*, 323.
- (2) (a) Lieber, C. M. *Solid State Commun.* **1998**, *107*, 607. (b) Alivisatos, A. P. *Science* **1996**, *271*, 933.
- (3) Kong, Y. C.; Yu, D. P.; Zhang, B.; Fang, W.; Feng, S. Q. *Appl. Phys. Lett.* **2001**, *78*, 407.
- (4) Li, Y.; Meng, G. W.; Zhang, L. D.; Phillip, F. *Appl. Phys. Lett.* **2000**, *76*, 2011.
- (5) Omichi, K.; Kaiya, K.; Takahashi, N.; Nakamura, T.; Okamoto, S.; Yamamoto, H. *J. Mater. Chem.* **2001**, *11*, 262.
- (6) Zu, P.; Tang, Z. K.; Wong, G. K.; Kawasaki, M.; Ohtomo, A.; Koinuma, H.; Segawa, Y. *Solid State Commun.* **1997**, *103*, 459.
- (7) Bagnall, D. M.; Chen, Y. G.; Zhu, Z.; Yao, T. *Appl. Phys. Lett.* **1997**, *70*, 2230.
- (8) Huang, M. H.; Mao, S.; Feick, H.; Yan, H. Q.; Wu, Y. Y.; Kind, H.; Weber, E.; Russo, R.; Yang, P. D. *Science* **2001**, *292*, 1897.
- (9) Yang, P.; Yan, H.; Mao, S.; Russo, R.; Johnson, J.; Saykally, R.; Morris, N.; Pham, J.; He, R.; Choi, H. *Adv. Funct. Mater.* **2002**, *12*, 323.
- (10) Pan, Z. W.; Dai, Z. R.; Wang, Z. L. *Science* **2001**, *292*, 1947.
- (11) Huang, M. H.; Wu, Y.; Feick, H.; Tran, N.; Weber, E.; Yang, P. *Adv. Mater.* **2001**, *13*, 113.
- (12) Yan, H.; He, R.; Pham, J.; Yang, P. *Adv. Mater.* **2003**, *15*, 402.
- (13) Hu, J. Q.; Bando, Y. *Appl. Phys. Lett.* **2003**, *82*, 1401.
- (14) Yan, H.; He, R.; Johnson, J.; Law, M.; Saykally, R. J.; Yang, P. J. *Am. Chem. Soc.* **2003**, *125*, 4728.
- (15) Hu, P.; Liu, Y.; Wang, X.; Fu, L.; Zhu, D. *Chem. Commun.* **2003**, 1304.
- (16) Sun, X. M.; Deng, Z. X.; Li, Y. D. *Mater. Chem. Phys.* **2003**, *80*, 366.
- (17) Gao, P.; Wang, Z. L. *J. Phys. Chem. B* **2002**, *106*, 12653.
- (18) Lao, J. Y.; Wen, J. G.; Ren, Z. F. *Nano Lett.* **2002**, *12*, 1287.
- (19) Lao, J. Y.; Huang, J. Y.; Wang, D. Z.; Ren, Z. F. *Nano Lett.* **2003**, *3*, 235.
- (20) Yamabi, S.; Imai, H. *J. Mater. Chem.* **2002**, *12*, 3773.
- (21) Vayssieres, L. *Adv. Mater.* **2003**, *15*, 464.
- (22) Zhang, B. P.; Binh, N. T.; Wakatsuki, K.; Segawa, Y.; Yamada, Y.; Usami, N.; Kawasaki, M.; Koinuma, H. *J. Phys. Chem. B* **2004**, *108*, 10899.
- (23) Lee, J. D. *Concise Inorganic Chemistry*, 4th ed.; Chapman & Hall: London, 1991; p 843.
- (24) Fu, Z.; Liu, B.; Liao, G.; Wu, Z. J. *Cryst. Growth* **1998**, *193*, 316.
- (25) Wu, J. J.; Liu, S. C. *Adv. Mater.* **2002**, *14*, 215.